Supplement of Nat. Hazards Earth Syst. Sci., 26, 6177–6198, 2026
https://doi.org/10.5194/nhess-26-6177-2026-supplement
© Author(s) 2026. CC BY 4.0 License.



Natural Hazards and Earth System Sciences
Open Access
EGU

Supplement of

Deep-learning prediction of high-frequency sea-level oscillations in the Adriatic Sea

Iva Međugorac et al.

Correspondence to: Iva Međugorac (iva.medugorac@gfz.hr)

The copyright of individual parts of the supplement might differ from the article licence.

S1 Detailed description of the $HFNet_{JE}$ model architecture

S1.1 Atmospheric encoder

The atmospheric encoder of the $HFNet_{JE}$ model (Fig. S1) processes all atmospheric variables jointly, enabling the network to learn interactions between variables and vertical levels directly. The atmospheric input consists of six variables (MSLP, T, r, u, v, and z), each represented as a tensor of size 96 × 1 × 56 × 72 (time × level × latitude × longitude) for MSLP and 96 × 4 × 56 × 72 for all other variables in ERA5, and 32 × 1 × 153 × 148 for MSLP and 32 × 4 × 153 × 148 for all other variables in CERRA. These variables are stacked along the channel dimension, forming an input tensor of size 96 × 6 × 4 × 56 × 72 for ERA5, and 32 × 6 × 4 × 153 × 148 for CERRA.

The input tensors are first processed by a block of four 3D convolutional layers, each followed by ReLU activation and 3D dropout. All convolutional layers use kernels of size 3 × 3 × 3 with stride and padding 1 × 1 × 1. The number of kernels increases progressively across the layers, with 24, 48, 96, and 160 kernels, respectively. The output of this block is then spatially downsampled using 3D max pooling with kernel size and stride 1 × 14 × 14.

The resulting feature tensor is subsequently processed by a custom 3D convolution applied only along the temporal dimension, using one shared kernel per channel (kernel size 5 × 1 × 1, padding 2 × 1 × 1), producing a feature tensor of size 640 × 96 × 4 × 5.

In the second stage (the temporal part of the encoder), the encoded features are processed by a series of temporal 3D convolutions with 192 kernels. This block begins with a 3D convolution with kernel size and stride 1 × 1 × 1, followed by two dilated convolutional units with residual connections. The first unit uses a 5 × 1 × 1 convolution with padding 4 × 0 × 0 and dilation 2 × 1 × 1, followed by SeLU activation, 3D dropout, and a 1 × 1 × 1 convolution to refine the feature representation. The second unit applies a 9 × 1 × 1 convolution with padding 8 × 0 × 0 and dilation 2 × 1 × 1, again followed by SeLU activation, 3D dropout, and a 1 × 1 × 1 convolution.

The resulting features (192 × 96) are then processed by two 1D convolutional layers with 192 kernels (kernel size 1). The second convolution is followed by SeLU activation, 1D dropout, and a residual connection. Finally, the atmospheric representation is projected using a dense layer with 256 units, followed by SeLU activation and dropout, producing a compact atmospheric feature vector.

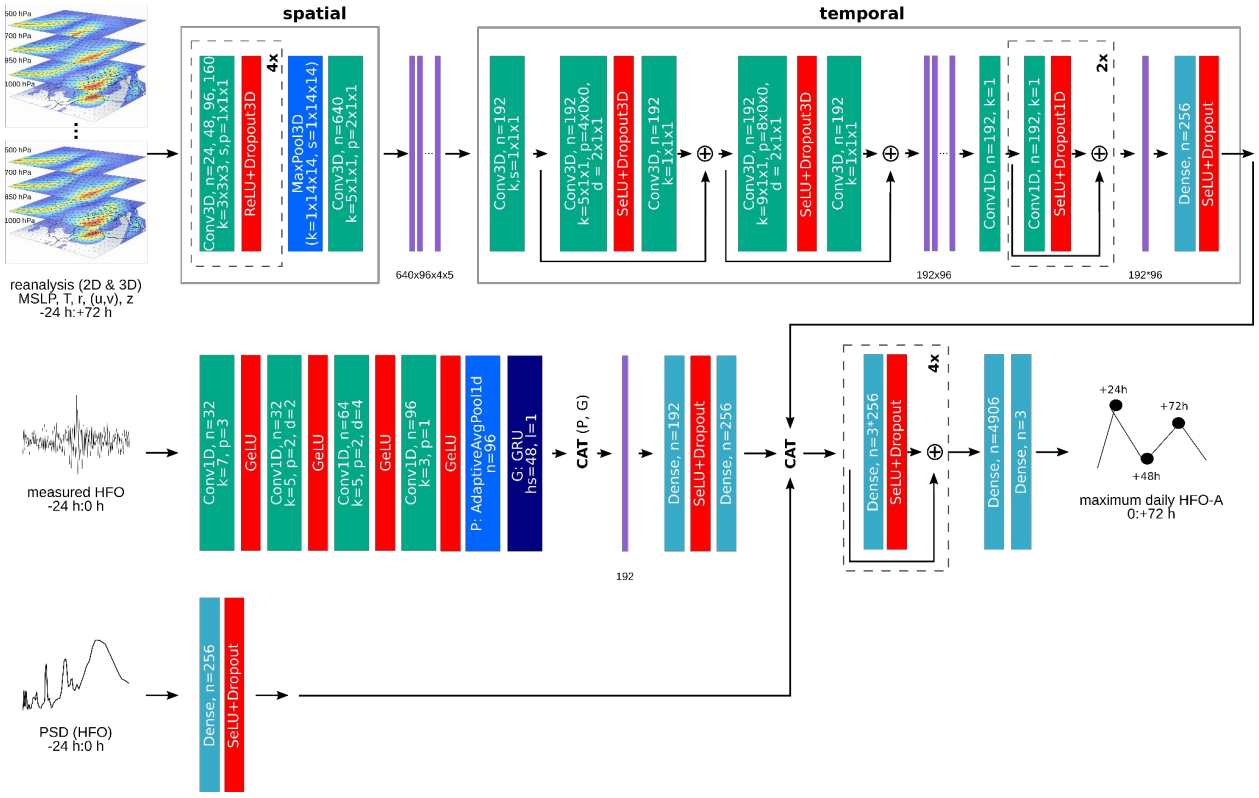


Figure S1. Architecture of the HFNet$_{JE}$ model. Colors indicate different layer types. *n* denotes the number of output channels, *k* the kernel size, *s* the stride, *p* the padding, *d* the dilation, *hs* the hidden size, *l* the layer.

S1.2 SL-data branches

The sea-level branch processes past HFO time series using a stack of 1D convolutional layers: Conv1D (32 kernels, size 7, padding 3), Conv1D (32 kernels, size 5, padding 2, dilation 2), Conv1D (64 kernels, size 5, padding 2, dilation 4), and Conv1D (96 kernels, size 3, padding 1). Each convolution is followed by GELU activation.

The extracted features are then reduced using adaptive average pooling to a fixed length of 96 and passed to a GRU layer (hidden size 48, single layer) to capture temporal dependencies. The outputs of the adaptive average pooling (P) and the GRU layer (G) are concatenated, forming a feature vector of size 192. This vector is subsequently processed through a fully connected layer, followed by SeLU activation and 1D dropout, and finally projected using a dense layer of size 256.

The PSD of past HFOs is incorporated through a third independent branch and projected using a fully connected layer of size 256 followed by SeLU and dropout.

S1.3 Fusion-regression block

The three feature vectors are then concatenated and processed by a regression block analog to that used in HFNet, consisting

of four residual blocks followed by two dense layers. Each residual block contains a fully connected layer that preserves the feature dimension (3·256), followed by SeLU activation and dropout, with a residual connection applied across the block. The resulting combined features are then mapped to a vector of size 4906 using a dense layer. Finally, a fully connected output layer produces the three target values, representing the predicted maximum daily HFO-A for the next three days.

S2 Ablation study for Bakar and Ploče

Table S1. Mean performance metrics averaged over three runs for station Bakar in the HFNet ablation experiments. Variants exclude individual predictors: $HFNet_{-PSD}$ (spectrum); $HFNet_{-Ri}$ (Richardson number); $HFNet_{-MSLP}$ (mean sea-level pressure); $HFNet_{-r}$ (relative humidity); $HFNet_{-HFO}$ (previous 24 hours of HFOs); $HFNet_{-T}$ (air temperature); $HFNet_{-(u,v)}$ (wind components); $HFNet_{-z}$ (geopotential). The reference HFNet model includes all predictors. Underlined values denote optimal values within each category (All, Reg, and Ext).

Experiment	Category	RMSE (cm)	MAE (cm)	Relative error (%)	Bias (cm)	Accuracy (%)
HFNet	All	3.15	2.22	41.87	0.90	88.95
$HFNet_{-PSD}$		3.04	2.22	43.2	0.86	89.50
$HFNet_{-Ri}$		<u>2.89</u>	<u>1.96</u>	<u>35.02</u>	<u>0.05</u>	<u>91.46</u>
$HFNet_{-MSLP}$		2.98	2.07	37.97	0.33	91.05
$HFNet_{-r}$		2.99	2.08	38.27	0.28	90.41
$HFNet_{-HFO}$		2.9	2.03	37.7	0.67	90.82
$HFNet_{-T}$		3.22	2.19	40.78	0.8	89.45
$HFNet_{-(u,v)}$		3.05	2.15	40.79	0.53	89.86
$HFNet_{-z}$		3.08	2.07	37.25	0.37	89.95
HFNet	Reg	2.88	2.11	42.19	1.04	89.93
$HFNet_{-PSD}$		2.72	2.09	43.49	1.03	90.77
$HFNet_{-Ri}$		<u>2.50</u>	<u>1.82</u>	<u>35.10</u>	<u>0.21</u>	<u>92.78</u>
$HFNet_{-MSLP}$		2.58	1.92	38.09	0.5	92.45
$HFNet_{-r}$		2.64	1.94	38.43	0.44	91.66
$HFNet_{-HFO}$		2.63	1.92	37.98	0.79	91.8
$HFNet_{-T}$		2.86	2.06	41.01	0.95	90.54
$HFNet_{-(u,v)}$		2.68	2.01	40.98	0.70	91.28
$HFNet_{-z}$		2.66	1.92	37.33	0.55	91.28

HFNet	Ext	9.20	7.46	26.53	-5.72	42.22
$HFNet_{-PSD}$		9.84	8.26	29.22	-7.49	28.89
$HFNet_{-Ri}$		10.29	8.69	31.27	-7.68	28.89
$HFNet_{-MSLP}$		10.69	9.03	32.22	-7.94	24.45
$HFNet_{-r}$		10.13	8.59	30.82	-7.06	31.11
$HFNet_{-HFO}$		<u>8.77</u>	<u>7.00</u>	<u>24.65</u>	<u>-5.39</u>	<u>44.44</u>
$HFNet_{-T}$		10.62	8.45	30.04	-6.63	37.78
$HFNet_{-(u,v)}$		10.41	8.84	31.66	-7.87	22.22
$HFNet_{-z}$		11.19	9.4	33.65	-8.17	26.67

Table S2. Mean performance metrics averaged over three runs for station Ploče in the HFNet ablation experiments. Variants exclude individual predictors: $HFNet_{-PSD}$ (spectrum); $HFNet_{-Ri}$ (Richardson number); $HFNet_{-MSLP}$ (mean sea-level pressure); $HFNet_{-r}$ (relative humidity); $HFNet_{-HFO}$ (previous 24 hours of HFOs); $HFNet_{-T}$ (air temperature); $HFNet_{-(u,v)}$ (wind components); $HFNet_{-z}$ (geopotential). The reference HFNet model includes all predictors. Underlined values denote optimal values within each category (All, Reg, and Ext).

Experiment	Category	RMSE (cm)	MAE (cm)	Relative error (%)	Bias (cm)	Accuracy (%)
HFNet	All	2.69	2.12	51.23	1.25	78.59
$HFNet_{-PSD}$		2.66	2.08	51.74	1.15	78.13
$HFNet_{-Ri}$		<u>2.42</u>	<u>1.84</u>	<u>43.07</u>	<u>0.75</u>	<u>82.03</u>
$HFNet_{-MSLP}$		2.56	2.01	48.9	1.06	79.83
$HFNet_{-r}$		2.59	1.97	46.51	0.84	81.57
$HFNet_{-HFO}$		2.65	2.06	49.43	1.21	79.78
$HFNet_{-T}$		2.54	1.93	45.25	0.84	80.88
$HFNet_{-(u,v)}$		2.57	2.01	49.04	1.01	80.38
$HFNet_{-z}$		2.64	2.03	48.32	1.04	79.92
HFNet	Reg	2.64	2.09	51.72	1.31	78.96
$HFNet_{-PSD}$		2.58	2.04	52.19	1.23	78.58
$HFNet_{-Ri}$		<u>2.34</u>	<u>1.8</u>	<u>43.37</u>	<u>0.82</u>	<u>82.64</u>
$HFNet_{-MSLP}$		2.48	1.97	49.29	1.13	80.35
$HFNet_{-r}$		2.5	1.93	46.86	0.92	82.07
$HFNet_{-HFO}$		2.6	2.04	49.9	1.28	80.12

$HFNet_{-T}$		2.45	1.89	45.59	0.92	81.47
$HFNet_{-(u,v)}$		2.5	1.96	49.43	1.09	80.91
$HFNet_{-z}$		2.55	1.99	48.68	1.13	80.45
HFNet		4.87	3.75	18.95	-2.99	54.54
$HFNet_{PSD}$		5.86	4.5	22.56	-4.36	48.48
$HFNet_{Ri}$		5.6	4.5	22.99	-3.56	42.42
$HFNet_{MSLP}$		5.77	4.65	23.58	-3.69	45.45
$HFNet_{r}$	Ext	5.94	4.71	23.95	-4.27	48.48
$HFNet_{HFO}$		4.81	3.75	18.91	-3.11	57.58
$HFNet_{T}$		5.81	4.57	23.19	-3.97	42.42
$HFNet_{(u,v)}$		5.57	4.6	23.69	-4.22	45.45
$HFNet_{z}$		6.22	4.86	24.49	-4.44	45.45

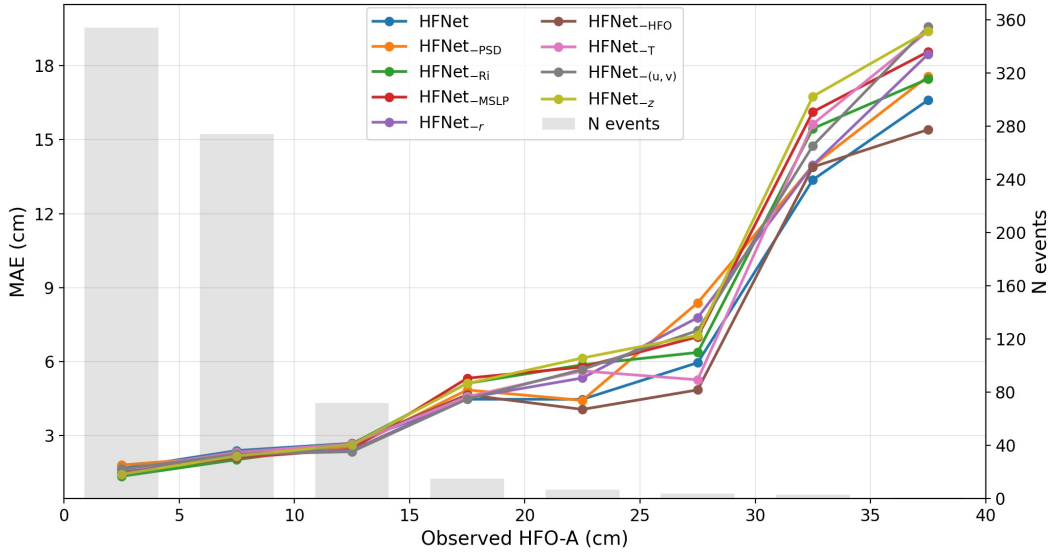


Figure S2. Mean MAE at the Bakar station for different amplitude bins and experiments with a 24-hour lead time. Each experiment was performed three times, and mean values are shown. Grey bars indicate the number of events in each bin.

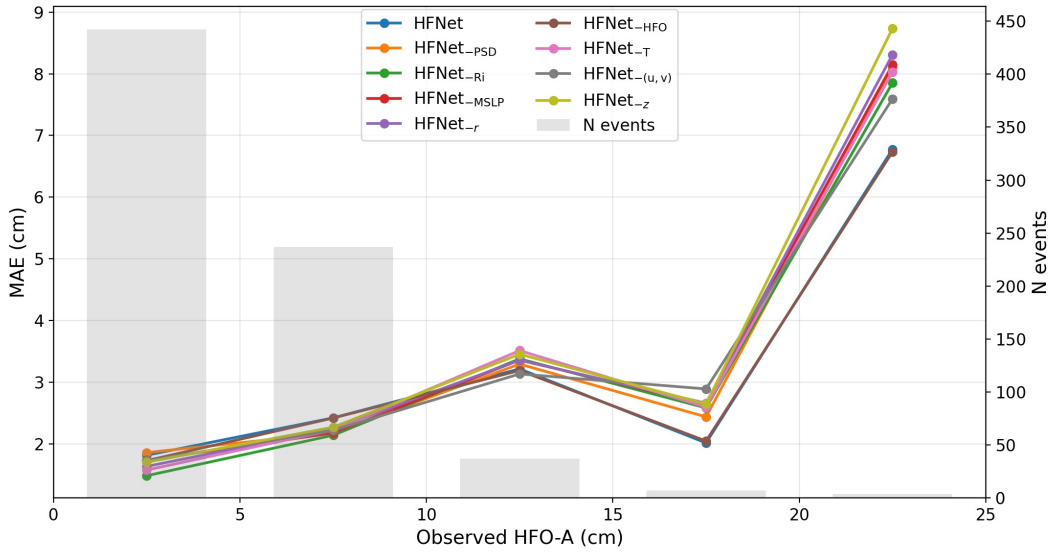


Figure S3. Mean MAE at the Ploče station for different amplitude bins and experiments with a 24-hour lead time. Each experiment was performed three times, and mean values are shown. Grey bars indicate the number of events in each bin.

S3 Prediction of HFOs using ECMWF forecasts (Ploče)

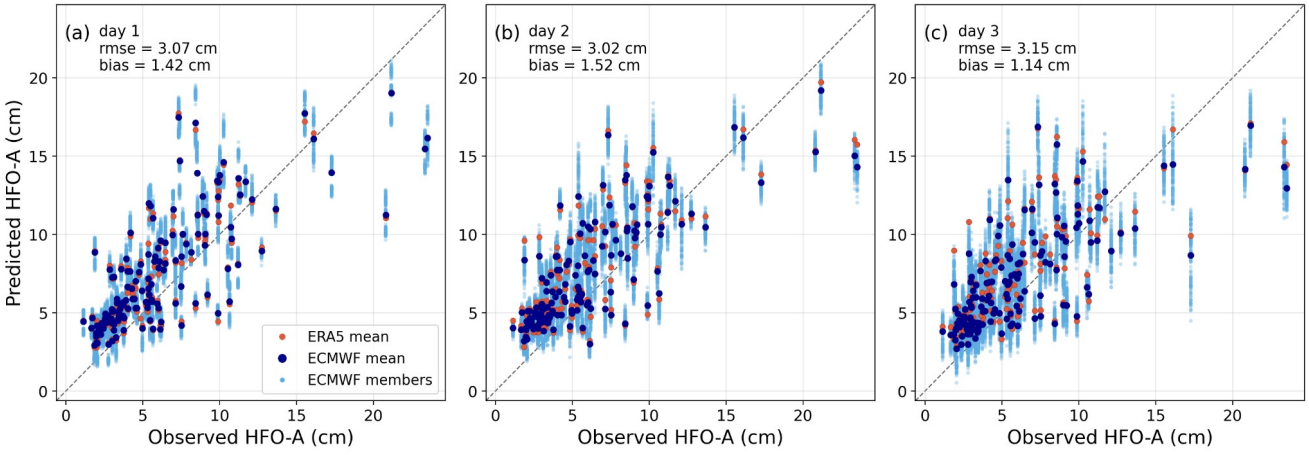


Figure S4. Scatter plots of observed and predicted HFO-A (model: $HFNet_{-HFO}$) at the Ploče station for August 2022 and July, August, October, and November 2023. Panels show lead times of (**a**) 24 hours, (**b**) 48 hours, and (**c**) 72 hours. Dark blue dots represent mean predictions from the 50-member ECMWF ensemble (averaged across three runs), red dots indicate corresponding means based on ERA5, and light blue dots show individual ECMWF ensemble members.

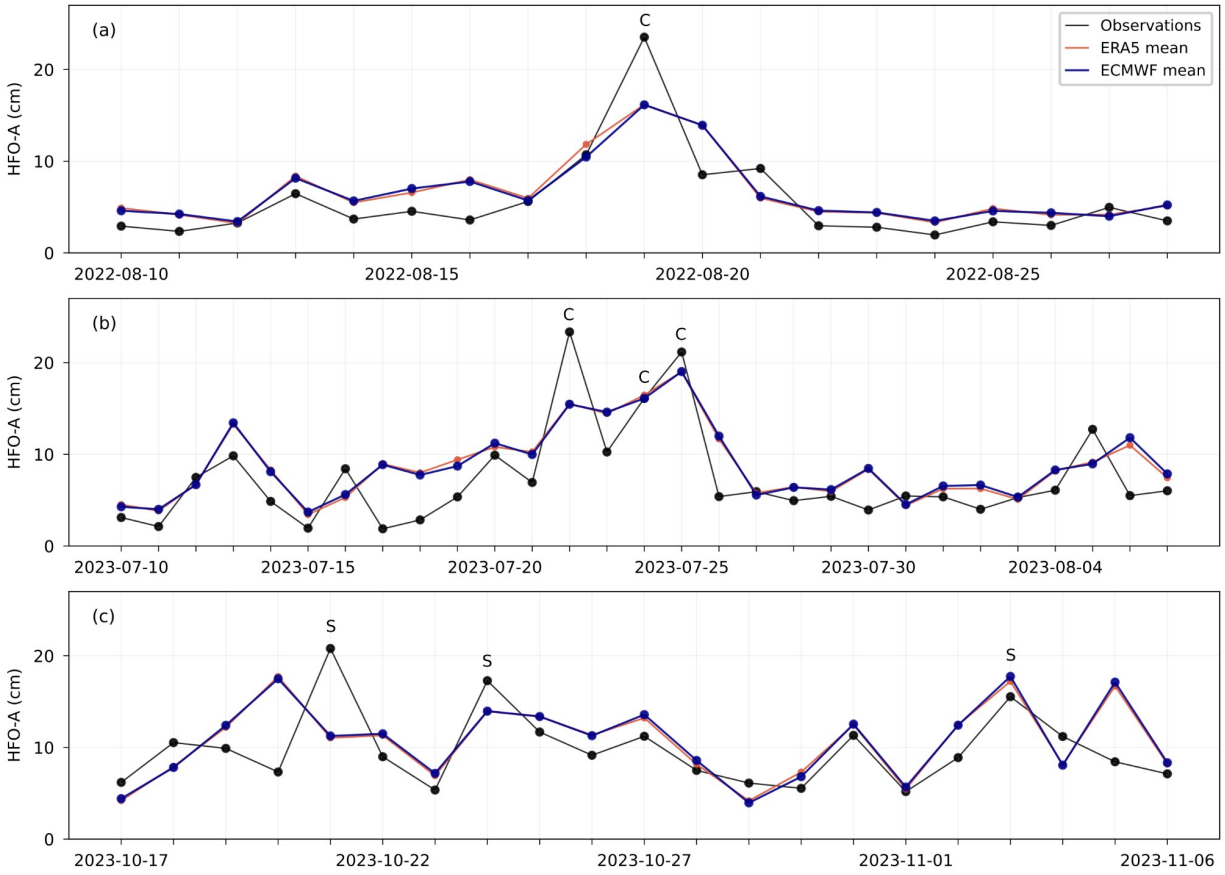


Figure S5. Time series of observed and predicted HFO-A at the Ploče station with a 24-hour lead time for selected periods: (**a**) August 2022, (**b**) July–August 2023, and (**c**) October–November 2023. Dark blue dots represent ensemble-mean predictions from the 50-member ECMWF forecasts (averaged across three runs), while red dots indicate the corresponding ERA5-based means. Letters marking observed values exceeding 15 cm denote the event class (see Section 4.1).